Veterinary Immunology and Immunopathology 152 (2013) 295–302

Contents lists available at SciVerse ScienceDirect

Veterinary Immunology and Immunopathology

journal homepage: www.elsevier.com/locate/vetimm

Research paper

Microsatellite $(GT)_n$ polymorphism at 3′UTR of SLC11A1 influences the expression of brucella LPS induced MCP1 mRNA in buffalo peripheral blood mononuclear cells

Sivamani Balasubramaniam, Subodh Kumar, Arjava Sharma, Abhijit Mitra*

Genome Analysis Laboratory, Division of Animal Genetics, Indian Veterinary Research Institute, Izatnagar, 243 122 Bareilly, India

ARTICLE INFO

Article history:
Received 10 September 2012
Received in revised form 8 December 2012
Accepted 28 December 2012

Keywords:
Buffalo
Chemokine
MCP1
SLC11A1
Brucellosis
PBMC

ABSTRACT

A $(GT)_n$ microsatellite polymorphism at 3′UTR of SLC11A1(solute carrier family 11A1) is associated with the natural resistance to bovine brucellosis. A pleiotropic effect of SLC11A1 on other candidate genes influencing the host resistance including monocyte chemotactic/chemoattractant protein 1 (MCP1) is also hypothesized. In the present study, we report the cloning and characterization of the complete coding sequence of bubaline (bu) MCP1 and its tissue distribution at the transcript level. The buMCP1 exhibited as high as 99% and >80% of sequence identities with the bovine and other domestic animal species homologues. The buMCP1 mRNA was abundant across the different tissues: most abundant in liver and mammary gland, moderate in ovary, skeletal muscle and testis, and least in uterus. Further, quantitative real-time PCR (RTqPCR) analysis revealed that PBMCs carrying so called resistant GT_{13} allele produced more MCP1 mRNA endogenously as well as when induced with brucella LPS suggesting the pleiotropic roles of SLC11A1 in conferring resistance against the intracellular pathogens particularly against brucellosis. However, the underlying molecular mechanisms by which 3′UTR SLC11A1 concomitantly increases the production of chemokines like MCP1 are yet to be investigated.

1. Introduction

SLC11A1 (solute carrier family 11A1), erstwhile referred as NRAMP1 (Natural Resistance Associated Macrophage Protein 1), regulates the macrophage function and thereby confers resistance to a number of antigenically different intracellular pathogens including *Brucella abortus* (Bradley et al., 1979; Gros et al., 1981; Plant and Glynn, 1974; Skamene et al., 1982). A (GT_n) microsatellite (where n is 13, 14, 15, or 16) polymorphism, located in the 3′UTR of bovine SLC11A1, has significant association with the natural resistance to brucellosis (Adams and Templeton, 1998). The susceptible mouse macrophage cell lines (RAW264.7) transfected with the bovine SLC11A1 resistant allele restricted the intracellular replication of *B. abortus* (Barthel et al., 2001). GT_n polymorphism has also been associated with the brucellosis resistance in buffalo (Borriello et al., 2006; Capparelli et al., 2007; Ganguly et al., 2008). The pleiotropic effect of SLC11A1 on other candidate genes influencing the host resistance is also hypothesized (Lang et al., 1997; Gazouli et al., 2008). Nevertheless, the independent roles of some of these candidate genes such as MCP1, TNF-alpha, TGF-beta, IL-10, IL-6 and IFN-gamma, E-selectin, L-selectin, and TLR4 have also been reported elsewhere (Eskra et al., 2003; Karaoglan et al., 2009; Rafiei et al., 2006, 2007; Rezazadeh et al., 2006).

Monocyte chemotactic/chemoattractant protein 1 (MCP1), a member of the C—C chemokine family, is expressed in a variety of cell types including endothelium, fibroblast, epithelium, smooth muscle, mesanglial, astrocyte, monocyte and microglial cells (Deshmane et al., 2009). However, monocytes are the major source of MCP1

* Corresponding author. Tel.: +91 581 2303382; fax: +91 581 2303284.
E-mail address: drabhijitmitra@gmail.com (A. Mitra).

0165-2427/$ – see front matter © 2013 Elsevier B.V. All rights reserved.
http://dx.doi.org/10.1016/j.vetimm.2012.12.015

(Yoshimura et al., 1989). The MCP1 has been associated with various inflammatory (Namiki et al., 2002; Spoettl et al., 2006; Ip et al., 2006) as well as few infectious diseases such as tuberculosis (Flores-Villanueva et al., 2005), paratuberculosis (Buza et al., 2003) and brucellosis (Eskra et al., 2003).

South and Southeast-Asian countries possess around 83% of the world buffalo (*Bubalus bubalis*) population of which India alone contributes 57%. Although numerically buffalo is just half the population of cattle, it contributes around 60% of the annual milk production of India (FAOSTAT, 2010). Further they are anecdotally referred as sturdy and resistant to various infectious diseases. A survey in India revealed 16.4% buffaloes were positive for brucellosis (Gwida et al., 2010). However, the fact that one fifth of animals still remain sero-negative even in a heavily infected herd (Borriello et al., 2006) necessitates the exploitation of the natural host resistance to brucellosis in buffaloes.

Since the discovery of human MCP1 (Yoshimura et al., 1989) its homologues have been cloned in different species including rabbit (Yoshimura and Yuhki, 1991), rat (Yoshimura et al., 1991), cattle (Wempe et al., 1991, 1994), guinea pig (Yoshimura, 1993), pig (Hosang et al., 1994) and sheep (Dunphy et al., 2001). However, bubaline MCP1 is yet to be characterized. In the present study, we cloned and characterized the complete coding sequence of bubaline MCP1 and further investigated the effect of SLC11A1 genotypes on the differential expression of MCP1 in PBMCs while induced with brucella LPS.

2. Materials and methods

2.1. Animals

Healthy adult female buffaloes ($n = 5$) belonging to Murrah breed maintained in the institute herd at Izatnagar (U.P.), India, were included in the study. All these animals were tested to be sero-negative for Rose Bengal Blue Test (RBPT), standard tube agglutination test (STAT) and indirect ELISA as described by Kumar et al. (2005). Further these animals had no history of abortion and vaccination against brucellosis.

2.2. Grouping of animals on the basis of GT_n genotypes

Genomic DNA was isolated from the venous blood using standard phenol chloroform extraction method (Sambrook et al., 1989). A region corresponding to 401 bp of 3′UTR of SLC11A1 was PCR amplified using the primers (forward: 5′-CGCTTCCTGTATGGGCTTC-3′ and reverse: 5′-TCCAAGGTAGGTGTCCCCA-3′) as described by Rajaravindra (2008). The amplified products were resolved by agarose gel (1%) electrophoresis and visualized using ethidium bromide (EtBr) staining under UV light. The PCR products were subjected to fragment analysis for microsatellite genotyping. The animals were classified into two groups based on their number of GT repeats present at the 3′UTR of SLC11A1 gene viz., GT_{13} (GT_{13}/GT_{13}) constituting of two animals homozygous for GT_{13} allele and NonGT_{13} (GT_n/GT_n, where $n \neq 13$) consisting of three animals carrying other than GT_{13} alleles in their homozygous form.

2.3. Isolation of PBMC

Venous blood (10 ml) was collected aseptically from the healthy adult animals. The peripheral blood mononuclear cells (PBMC) were separated by density gradient centrifugation using Hisep (Himedia, India) following manufacturer's instructions. Briefly, 8 ml of PBS-diluted (1:1) blood samples were layered over 4 ml of Hisep in 15 ml tube and centrifuged at $400 \times g$ for 30 min. The PBMCs aggregated at the interphase were collected and washed three times with sterile PBS.

2.4. Induction of PBMC culture

Following the adjustment of concentration of PBMC to 5×10^6 cells per ml, the PBMC were cultured in a 25 ml tissue culture flask for 30–36 h using RPMI 1640 cell culture medium (Sigma, USA) supplemented with 10% heat inactivated Fetal Calf Serum (Sigma, USA) and antibiotics Penicillin G (100 IU/ml) and Streptomycin (100 μg/ml). The PBMC of animals belong to both the genotype groups were induced with the LPS derived from *B. abortus* strain-99 (OIE Manual, 2004) at a final concentration of 0 and 20 μg/5×10^6 cells for 12 h.

2.5. cDNA synthesis

The total RNA was isolated from PBMCs using Trireagent (Sigma, USA) according to the manufacturer's instructions. The isolated RNA sample was treated with DNase using DNA-free™ DNase Treatment & Removal Reagents (Ambion, USA). The concentrations and purities of RNA preparations were determined spectrophotometrically at OD260 and OD280. The total RNA was reverse-transcribed using Reverse Transcription (RT) System (Promega, USA) following the manufacturer's instructions. Briefly the cDNA was synthesized from approximately 2 μg total RNA using oligo-dT primers and avian myloblastosis virus reverse transcriptase in a final volume of 20 μl. The resultant first strand of cDNA was stored at −20 °C until use.

2.6. PCR amplification of MCP1

A complete coding region of MCP1 was amplified using a pair of MCP1 specific primers (forward: 5′-CCAACAGCTTCCACGCTGAAAC-3′ and reverse: 5′-GCAGTTAGGGAAAGCCGGAAGA-3′). PCR amplification was carried out in a total volume of 25 μl that contained 7.5 pmol of each primer, 1 μl of cDNA, 10 mM Tris–HCl (pH 8.8), 50 mM KCl, 2.0 mM $MgCl_2$, 2.5 mM of each dNTPs and one unit of *Taq* DNA polymerase (Fermentas, USA). The amplification was carried out in a Thermal Cycler (Eppendorf, Germany) in the following cycling conditions: it included an initial period of denaturation at 94 °C for 2 min, followed by 35 cycles of denaturation at 94 °C for 30 s, annealing at 58 °C for 30 s and extension at 72 °C for 45 s, and a final extension at 72 °C for 10 min. The PCR

amplified products were resolved by agarose gel (1%) electrophoresis and visualized using ethidium bromide (EtBr) staining under UV light.

2.7. Cloning and sequencing

The amplicon of MCP1 was cloned into pGEMT Easy vector (Promega, USA) following the manufacturer's instructions. Positive recombinant clones were identified using blue and white screening. Further, the presence of the insert was confirmed by restriction digestion with EcoRI and PCR amplification of the insert using recombinant plasmid as a template. The positive clones were sequenced using an automated sequencer using Sanger's dideoxy chain termination method with the standard T7 and SP6 sequencing primers.

2.8. Public sequence used

In addition to the buMCP1 sequenced in the present study, coding sequences of the several mammalian species available in GenBank database were also included; Indian cattle (EU837194), taurine cattle (EU276059), pig (EU682328), horse (EU438774), dog (NM_001003297), human (NM_002982), crab eating macaque (AF276081), olive baboon (NM_001173538), pig tailed macaque (AY206693), rabbit (NM_001082294), rhesus monkey (NM_001032821), Sumatran orangutan (NM_001132340), mouse (NM_011333), rat (NM_031530.1), guinea pig (NM_001172926.1), and Hispid cotton rat (AF165953).

2.9. Sequence analysis

The sequences were subjected to BLAST analysis (http://www.ncbi.nlm.nih.gov/BLAST). The nucleotides as well as the deduced amino acid sequences were aligned with those of available species in the GenBank database using the Clustal method of MegAlign Programme of Lasergene Software (DNASTAR, USA). Phylogenetic and molecular evolutionary analyses were conducted using *MEGA* version 4 (Tamura et al., 2007). Phylogenetic tree was constructed using neighborhood joining method. Reliability of a tree obtained was tested by bootstrapping test of phylogeny. Ratios between synonymous and non-synonymous substitutions (ω) along AA sites were estimated with the program codeml of the PAML package, using model M3, with $K = 3$ AA site classes as in Yang et al. (2000). Signal peptide of the sequences was predicted by SignalP 4.0 server http://www.cbs.dtu.dk/services/SignalP/ (Petersen et al., 2011). The isoelectric point and the molecular weight of deduced peptide were predicted using the expasy tools (http://expasy.org/cgi-bin/protparam). The domain features of deduced buMCP1 were determined by ScanProsite of expasy tools. O-linked glycosylation, N-linked glcosylation, phosphorylation sites and disulfide bonds were predicted using YinOYang 1.2 tool, NetNGlyc 1.0 server, http://www.predictprotein.org and DiANNA web server 1.1, respectively.

2.10. Expression of buMCP1 in various tissues using semi-quantitative PCR

Total RNA was extracted from approximately 100 mg of each tissue including liver, mammary gland, skeletal-muscle, ovary, testis and uterus were collected upon slaughter from apparently healthy adult buffalo from the local abattoir. Two micrograms of total RNA from each sample was reverse transcribed as described above. Exactly 1 μl of cDNA of all tissues was subjected to PCR using MCP1 PCR primers as described under Section 2.6. GAPDH was used as an internal control to assess the variations in the efficiencies of the RT step among different experimental samples. A 496 bp fragment of GAPDH was amplified independently using a pair of primers (forward: 5′-CAAGGTCATCCATGACAACTTTG-3′; reverse: 5′-GTCCACCACCCTGTTGCTGTAG-3′). For amplification of GAPDH gene, the same reaction conditions and components as described for the amplification of buMCP1 gene were used. In order to check the DNA contamination for each RNA sample, a control reaction was set up in which reverse transcriptase enzyme was omitted during cDNA synthesis. The number of cycles used to amplify the cDNA of both the genes was kept identical. Each PCR mixture (8 μl) was electrophoresed through EtBr stained 1.0% agarose gel and photographed using gel-documentation system (Syngene, USA). The size of PCR products was verified by comparing with a DNA Ladder (SM #1173; Fermentas, USA). The concentrations of the GAPDH and buMCP1 mRNA were determined by densitometry analysis (Tan and Ng, 2008) using ImageJ software (ImageJ, version 1.46 g, NIH, USA). In brief, the gel image to be analyzed (TIF format) is opened with ImageJ and converted to 8bit format. Then the background is subtracted using rolling ball radius option. The bands are selected by rectangle tool and the lanes are plotted using plot lanes option. Once the plotted lanes are selected through line and wand tools the area is displayed corresponding to their band intensity and size. The relative expression was determined as arbitrary units, defined as the ratio of mRNA level of MCP1 to the corresponding GAPDH mRNA level [value = (area of MCP1)/(area of GAPDH)].

2.11. Expression of MCP1 in different genotypes of SLC1A1 using quantitative real-time PCR (RTqPCR)

The total RNA was isolated from the induced and uninduced PBMCs of different genotype groups and was subsequently reverse transcribed as described above. The gene-specific real-time primers for MCP1 (forward 64F: 5′-CTCGCTCAGCCAGATGCAA-3′ and reverse 173R: 5′-TTGCTGCTGGTGACTCTTCTGT-3′) and endogenous control GAPDH (forward F: 5′-CTCCTGCACCACCAACTG-3′ and reverse R: 5′-CGCCAGTAGAAGCAGGGA-3′) were designed using Primer Express (Ver3.0) on the basis of available cDNA sequences in the GenBank.

To avoid non-specific amplification and primer–dimers in quantitative expression of MCP1 and GAPDH the specific combinations of forward and reverse primers were selected through primer optimization matrix (Mikeska and Dobrovic, 2009). In the present study MCP1 specifically

amplified at 50:50 nmol/l and GAPDH at 100:50 nmol/l of forward and reverse primer combinations. The PCR efficiency (E) for MCP1 and GAPDH was found to be 101.8 and100 percentages, respectively.

Then, the RTqPCR was carried out on cDNA samples using Applied Biosystems (ABI7500) real-time PCR System. All PCR reactions were performed in 20 μl volume in duplicates. The reaction mixture contained 1× SYBR® Green Master Mix (Applied Biosystems, USA) 5 μl of cDNA (1:10 diluted) template and gene specific primers along with one no template control for each gene. The thermo-cycling conditions were: 50 °C for 2 min, 95 °C for 10 min, followed by 40 cycles of 95 °C for 15 s and 60 °C for 1 min. The dissociation reaction was carried out under following cycling conditions. They were 1 cycle of 95 °C for 15 s, 60 °C for 1 min, 95 °C for 15 s and 60 °C for 15 s. The observed C_T values were used to calculate the relative quantitation (RQ) using the comparative C_T method (Livak and Schmittgen, 2001).

2.12. Nitric oxide estimation

The nitric oxide (NO) production by PBMCs after stimulation with *B. abortus* LPS was measured using colorimetric assay kit (Cayman Chemicals, Item No. 780001, USA) following the manufacturer's instructions.

2.13. Statistical analysis

Gene expression fold change values obtained from RT-qPCR were log transformed to normalize the data. Subsequently, differences between the groups for MCP1 expression and NO production were statistically analyzed by one way ANOVA (SPSS16.0). All numerical data were expressed as a mean ± SE.

3. Results

3.1. Sequence analysis of buMCP1

A 405 bp fragment of buMCP1 cDNA (Fig. 1), comprising of the complete coding sequence (CDS) of 300 bp, was cloned and sequenced. Blast analysis of the obtained sequence revealed >80% identity with the MCP1 sequences of domestic animal species available in the GenBank. Accordingly, the buMCP1 sequence was submitted in the GenBank under the Acc No. HQ889748.

3.2. MCP1 expression in various tissues

The MCP1 mRNA was the most abundant in the liver and mammary gland tissues. The expression of MCP1 was moderate in the ovary, skeletal muscle and testis, and was the least in the uterus (Fig. 2).

3.3. Differential expression of MCP1 in PBMC

The differential expression of MCP1 was observed in the PBMC of different genotype groups (Fig. 3). There were five folds more ($P < 0.01$) endogenous expression of MCP1 mRNA in the PBMC of GT_{13} animals compared to $NonGT_{13}$

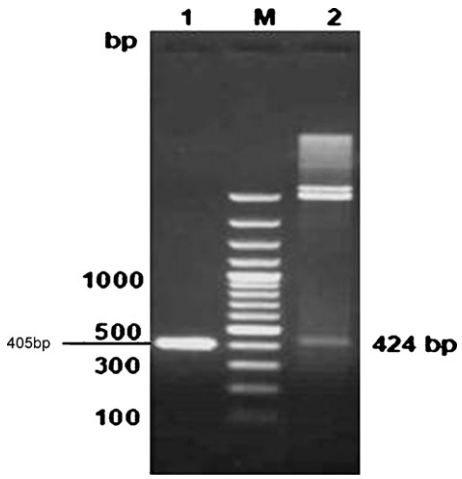

Fig. 1. Amplification of 405 bp fragment of MCP1 using recombinant plasmid as a template (lane 1) and restriction enzyme (EcoRI) digestion of recombinant plasmid (lane 2) showing the release of the MCP1 insert of 424 bp. Lane M: 100 bp DNA ladder.

LPS induction further potentiated the MCP1 mRNA expression by 2.5 times ($P < 0.01$) in the PBMCs of GT_{13} group (Fig. 3) with no effect ($P = 0.511$) on $NonGT_{13}$ group.

3.4. NO production

The amount of NO production did not differ markedly in the PBMC of different genotypic groups.

4. Discussions

4.1. Characterization of buMCP1

We have cloned the CDS (300 bp) of buMCP1 which encodes MCP1 peptide comprising of 99 amino acids having the molecular weight of 11.1 Kda and predicted isoelectric pH of 9.5. Like bovine, swine, equine and primates,

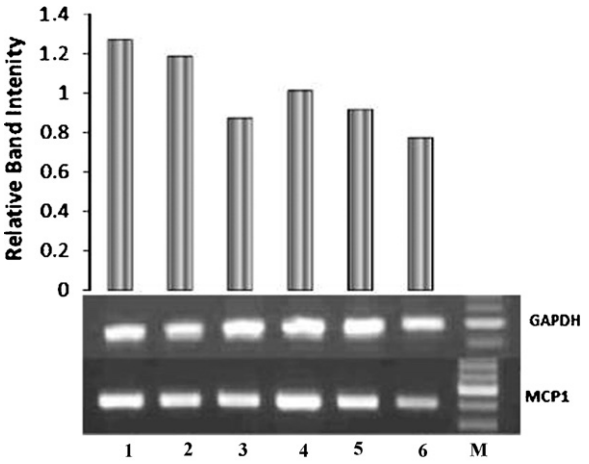

Fig. 2. Relative mRNA expression of buMCP1 in buffalo tissues. RT-PCR amplified products of bu-GAPDH and buMCP1 from different tissues viz., liver (lane 1), mammary gland (lane 2), skeletal muscle (lane 3), ovary (lane 4), testis (lane 5) and uterus (lane 6), 100 bp DNA marker (M).

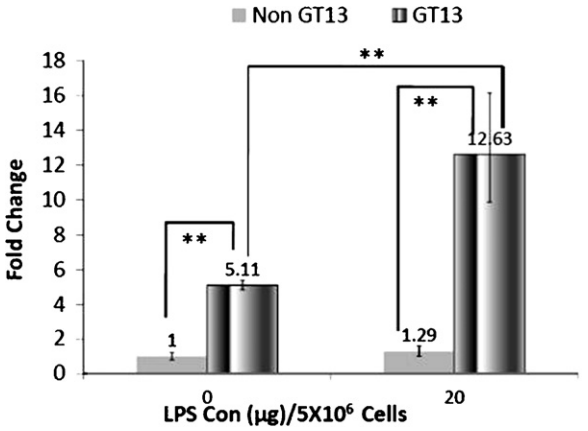

Fig. 3. Expression of buMCP1 in GT_{13} ($n=2$) and $NonGT_{13}$ ($n=3$) genotype groups upon induction with Brucella LPS at concentrations of 0 and 20 μg/5 × 10^6 cells.

the size of the buMCP1 CDS is conserved. However, CDS is longer in dog, rodents and rabbit. The MCP1 peptide of dog possesses two additional amino acids at the positions of 93 and 94. In rodents (guinea pig-120, mouse-148, rat-148 and Hispid cotton rat-150 amino acids) and rabbit (125 amino acids), excess amino acids are present at the carboxyl terminal of the peptide. The MCP1 protein is highly conserved at the N terminus among different species whereas C terminus remains much more variable (Yao and Tsirka, 2010).

The buMCP1 protein possesses a signal peptide of 23 amino acids which is predicted to be cleaved between Ala and Gln residues to yield the mature buMCP1 peptide (76 amino acids) of 24th to 99th amino acid residues. The signal peptide length and the first four amino terminal residues (QPDA) of the mature peptide are conserved in all the species (Yoshimura, 1993) (except guinea pig which has G at the fourth place) analyzed under the present study. The predicted secondary structure of peptide shows around 39.4% helical, 18.2% strand and 42.4% loop with a C-terminal α helical stretch.

The deduced amino acid sequence of bu-MCP1 exhibited the sequence identity of 100% and 99% with that of Indian and taurine cattle. Alignment report of the deduced amino acids (Fig. 4) of the Bovidae species indicated only one amino acid change at 69th position having *Val* in Indian cattle and buffalo, and *Ile* in taurine cattle. The other domestic animal species including pig, horse and dog exhibited 83.8, 79.8 and 73.7% identities, respectively. At amino acid level, the Cercopithecidae family of primates exhibited 72.7% identity whereas the Hominidae family exhibited 70.7% only. Rodents exhibited the least identities (50–55%) with that of buMCP1 peptide.

The phylogenetic tree constructed based on nucleotides (Fig. 5) and deduced amino acids (not shown) sequences revealed similar trend. buMCP1 formed a single clad with Indian and taurine cattle. The next nearer branches are formed by pig (87.3%) and horse (84.3%). The order carnivora including dog and American mink showed the identity of around 83% with the buMCP1. The primates formed a separate clad with the identity of around 81–83%. The primate clad is further separated into two branches; Cercopithecidae family (crab eating macaque, pig tailed macaque and rhesus monkey) and Hominidae family (human and orangutan). The order rodentia including mouse, guinea pig, rat and Hispid cotton rat exhibited the identity of 65 to 73%. The dN/dS analysis revealed that 24 out of 99 amino acids showed dN/dS ratio of >1 indicating positive selection pressure. Among them eight amino acids at positions of 20, 45, 49, 69, 71, 88, 89 and 99 received the highest score ranging from 0.983 to 1.0.

Structure-function studies demonstrated the importance of the N-terminal region of MCP1 in receptor binding and activation (Clark-Lewis et al., 1991). The rodent MCP1 C-terminus is decorated extensively with O-linked glycosylation sites (Zhang et al., 1996), which promotes the formation of dimer or higher order aggregates of MCP1. It is then cleaved by plasmin during cell injury and thus abrogates the dimer, make them easily diffuse in the cell and bind efficiently CCR2. The plasmin-regulated extracellular cleavage step is a functional characteristic for other chemokines such as cCAF (chicken chemotactic and angiogenic factor) and the hemofiltrate CC chemokine 1 (Vakili et al., 2001; Martins-Green, 2001). For primates and domestic animals, the MCP-1 gene seems to have evolved to lose this regulatory cleavage step since they lack the C-terminal extension (Yao and Tsirka, 2010). Yoshimura and Yuhki (1991) demonstrated that the sequence motif YXR (positions 51–53) dictates the receptor specificity of the MCP1 molecules. We and others (Hosang et al., 1994) found the 52nd residue X to be a basic in all the species with the exception of guinea pig.

The 34–76 amino acids of buMCP1 peptide represent the signature sequence of small cytokine C—C subfamily. The conserved *Cys* residues were observed at the positions of 34, 35, 59 and 75 in all the species including rodents and they were predicted (DiANNA web server 1.1) to form disulfide bridges at *Cys* 34–59 and *Cys* 35–75. The YinOYang 1.2 tool revealed the most probable sites of O-linked glycosylation for *Thr* at the positions of 19, 55 and 96 and *Ser* at 4 and 56. However, we could not detect any putative N-linked glycosylation sites as reported by Dunphy et al. (2001) in ovine. Ruggiero et al. (2003) proposed that differential glycosylation may allow highly effective short-lived MCP1 or less-effective long-lived MCP1 to be obtained, and may thus represent a novel mechanism of adaptation to pathological versus physiological conditions. A PROSITE database search of predicted protein identified two putative cAMP and cGMP-dependent protein kinase phosphorylation sites, three protein kinase-C phosphorylation sites and a tyrosine kinase phosphorylation site. Whereas Dunphy et al. (2001) reported one putative cAMP/cGMP kinase site and two protein kinase C sites in sheep.

4.2. MCP1 expression and NO production between genotype groups

MCP1 regulates the migration and infiltration of immune response cells to the infected sites and thus overcome the infection. It is expressed in a variety of cells including endothelium, epithelium and smooth muscle.

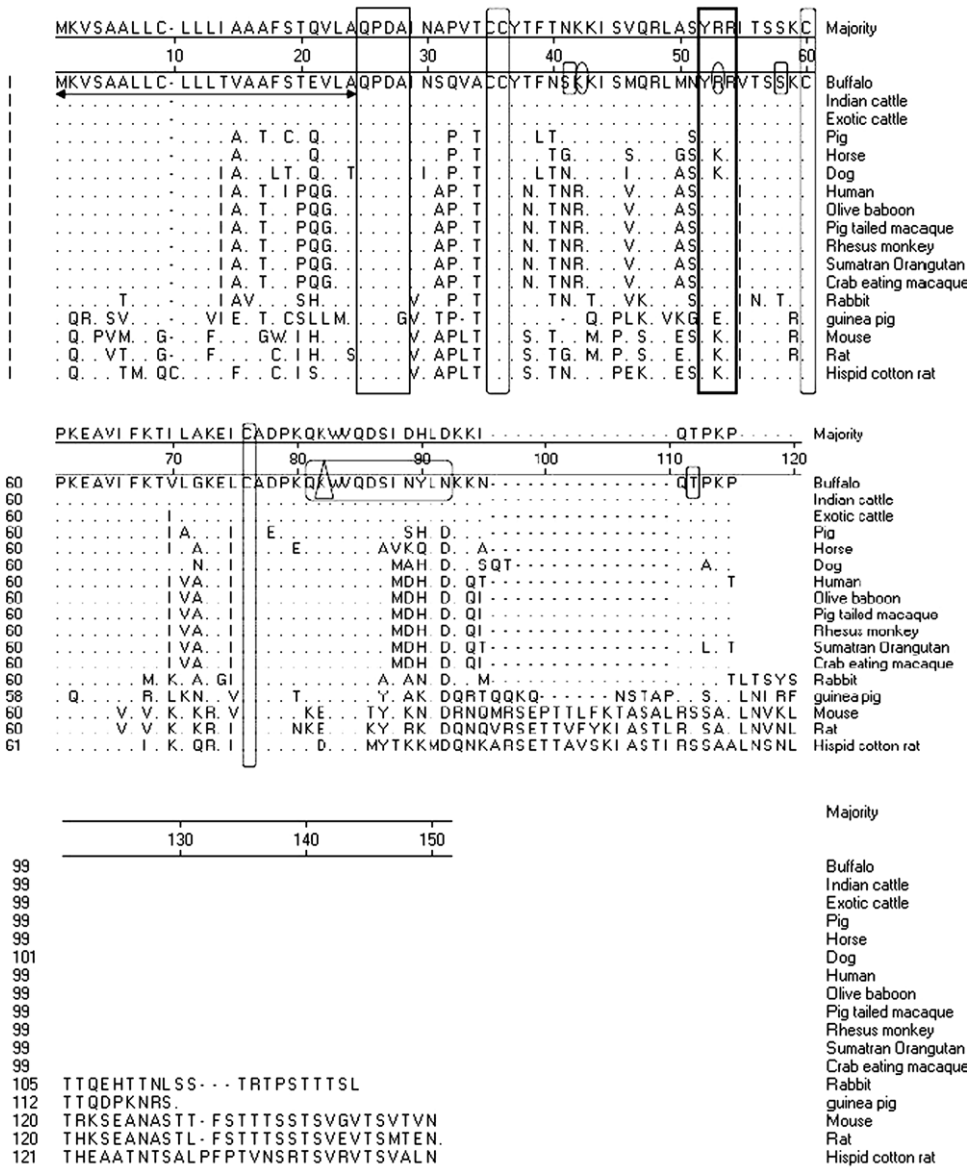

Fig. 4. Alignment report of deduced amino acid sequence of buMCP1 with that of other species. The dots indicate the same residues with that of buffalo. The double edged arrow (↔) indicates the signal peptide of buMCP1. The rectangle covering the QPDA at the positions of 24–27 residues (next to the signal peptide) indicates the conserved N-terminal mature peptide in all the species. The smooth rectangles at the positions of 34–35; 59 and 75 indicate the conserved cysteine residues. The thick rectangle (51–53) indicates the conserved residues which dictate the receptor specificity. The smooth rectangle encircling the 80–91 residues indicates the C-terminal α helix. Two small elliptical curves at the positions of 41 and 52 indicate cAMP and cGMP dependent protein kinase phosphorylation sites. Three small smooth rectangles indicate (at 40, 56 and 96) the protein kinase c phosphorylation site. One small triangle (at 81) indicates tyrosine kinase phosphorylation site.

The mRNA expression across various tissues of buffalo, observed in the present study, is suggestive of its role in mounting an immune and inflammatory response against infection (Rodríguez-Sanabria et al., 2010).

Host-resistance to intracellular pathogens is mediated through a complex process. SLC11A1 is known to play a major role in conferring resistance against intracellular pathogens (Skamene et al., 1982). The SSCA analysis (Adams and Templeton, 1998) and transfection study (Barthel et al., 2001) proved the association of 3′UTR microsatellite polymorphism with brucellosis resistance. In contrast, some reports refuted any association of 3′UTR polymorphism with the host resistance to *Brucella meletensis* in mice (Guilloteau et al., 2003) and *B. abortus* in cattle (Kumar et al., 2005; Paixao et al., 2007). Nevertheless, in buffalo, we and others established the association of GT_n polymorphism with the brucellosis resistance (Borriello et al., 2006; Capparelli et al., 2007; Ganguly et al., 2008). In our previous studies, we further demonstrated that the PBMC from GT_{13} animals produced significantly more H_2O_2

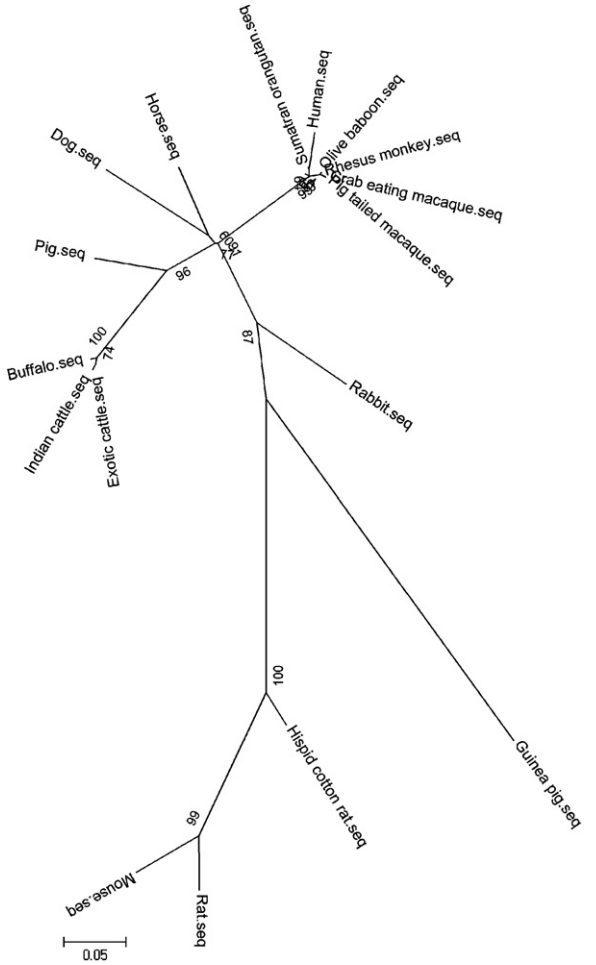

Fig. 5. Phylogenetic tree constructed on the basis of nucleotide sequence of buffalo MCP1 gene with that of other species.

and NO than those from $NonGT_{13}$ animals while induced with brucella LPS (Ganguly et al., 2008; Rajaravindra, 2008). It is also believed that SLC11A1 might exert pleiotropic effects on innate immune functions by modulating the production of chemokines, cytokines and the formation of reactive oxygen and nitrogen species (Valdez et al., 2008). Accordingly, we intended to evaluate whether PBMCs from buffaloes having so called resistant GT_{13} allele produce more MCP1 when compared to $NonGT_{13}$. We demonstrated that PBMCs carrying GT_{13} allele produced more MCP1 mRNA endogenously as well as when induced with brucella LPS. However, we could not detect any changes in the NO production between genotype groups. It might be due to the fact that the PBMC culture was induced with brucella LPS only for 12 h. Several studies (Wang et al., 1994; López-urrutia et al., 2000) also revealed that the measurable change of NO production between different groups could be observed during 24–48 h. But, as we are more interested in the mRNA level of MCP1 only, we did not extend the PBMC culture for longer duration. However it will be interesting to see the NO level at different time intervals.

5. Conclusion

In conclusion this is the first ever study reporting the cloning, characterization and expression profile of buMCP1. The microsatellite polymorphism at 3′UTR of SLC1A1 significantly influences the MCP1 expression in PBMC suggesting the pleiotropic roles of SLC11A1 in conferring resistance against the intracellular pathogens particularly against brucellosis. However, the underlying molecular mechanisms by which 3′UTR SLC11A1 concomitantly increases the production of chemokines (MCP1) are yet to be investigated.

Acknowledgements

This work was carried out under the project supported by IVRI (ICAR) IRC Research Grant given to AM as a Principal Investigator. Financial Assistance provided to SB in the form of Institute (IVRI) PhD fellowship is duly acknowledged. The authors are grateful to Dr. A. K. S Tomar (Senior Scientist) of Livestock Production & Management Section, IVRI for providing blood samples, to Dr. D.K. Singh (Principal Scientist, Division of Veterinary Public Health, IVRI) and to Dr. Rajesh Rathore (Senior Scientist, CADRAD, IVRI) for providing the facilities to serotype the animals.

References

Adams, L.G., Templeton, J.W., 1998. Genetic resistance to bacterial diseases of animals. Rev. Sci. Tech. 17, 200–219.

Barthel, R., Feng, J., Piedrathia, J.A., McMurray, D.N., Templeton, J.W., Adams, G.L., 2001. Stable transfection of the bovine NRAMP1 gene into murine RAW264.7 cells: effect on *Brucella abortus* survival. Infect. Immun. 69, 3110–3119.

Borriello, G., Capparelli, R., Bianco, M., Fenizia, D., Alfano, F., Capuano, F., Ercolini, D., Parisi, A., Roperto, S., Iannelli, D., 2006. Genetic resistance to *Brucella abortus* in the water buffalo (*Bubalus bubalis*). Infect. Immun. 74 (4), 2115–2120.

Bradley, D.J., Taylor, B.A., Blackwell, J., Evans, E.P., Freeman, J., 1979. Regulation of leishmania populations within the host. III. Mapping of the locus controlling susceptibility to visceral leishmaniasis in the mouse. Clin. Exp. Immunol. 37, 7–14.

Buza, J.J., Mori, Y., Bari, A.M., Hikono, H., Aodon-geril, Hirayama, S., Shu, Y., Momotani, E., 2003. Mycobacterium avium subsp. paratuberculosis infection causes suppression of RANTES, monocyte chemoattractant protein 1, and tumor necrosis factor alpha expression in peripheral blood of experimentally infected cattle. Infect. Immun. 71 (December (12)), 7223–7227.

Capparelli, R., Alfano, F., Amoroso, M.G., Borriello, G., Fenizia, D., Bianco, A., Roperto, S., Roperto, F., Iannelli, D., 2007. Protective effect of the nramp1 BB genotype against *Brucella abortus* in the Water Buffalo (*Bubalus bubalis*). Infect. Immun. 75 (2), 988–996.

Clark-Lewis, I., Schumacher, C., Baggiolini, M., Moser, B., 1991. Structure activity relationships of interleukin-8 determined using chemicallysynthesized analogs. Critical role of NH2-terminal residues and evidence for uncoupling of neutrophil chemotaxis, exocytosis,and receptor binding activities. J. Biol. Chem. 266, 23128–23134.

Deshmane, S.L., Kremlev, S., Amini, S., Sawayal, B.E., 2009. Monocyte chemoattractant protein-1 (MCP-1): an overview. J. Interferon Cytokine Res. 29 (6), 313–326.

Dunphy, J., Horvath, A., Barcham, G., Balic, A., Bischof, R., Meeusen, E., 2001. Isolation, chracterisation and expression of mRNAs encoding the ovine CC chemokines, monocyte chemoattractant protein (MCP)-1α and -2. Vet. Immunol. Immunopathol. 82, 153–164.

Eskra, L., Mathison, A., Splitter, G., 2003. Microarray analysis of mRNA levels from RAW264.7 macrophages infected with *Brucella abortus*. Infect. Immun. 71 (3), 1125–1133.

FAOSTAT, 2010, http://faostat.fao.org

Flores-Villanueva, P.O., Ruiz-Morales, J.A., Song, C.H., Flores, L.M., Jo, E.K., Montano, M., Barnes, P.F., Granados, S.M., 2005. A functional promoter polymorphism in monocyte chemoattractant ppotein-1 is associated

with increased susceptibility to pulmonary tuberculosis. J. Exp. Med. 202, 1649–1658.
Ganguly, I., Sharma, A., Singh, R., Deb, S.M., Singh, D.K., Mitra, A., 2008. Association of microsatellite $(GT)_n$ polymorphism at 3′UTR of NRAMP1 with the macrophage function following challenge with Brucella LPS in buffalo (*Bubalus bubalis*). Vet. Microbiol. 129, 188–196.
Gazouli, M., Atsaves, V., Mantzaris, G., Economou, M., Nasioulas, G., Evangelou, K., Archimandritis, A.J., Anagnou, N.P., 2008. Role of functional polymorphisms of NRAMP1 gene for the development of Crohn's disease. Inflamm. Bowel Dis. 14 (10), 1323–1330.
Gros, P., Skamene, E., Forget, A., 1981. Genetic control of natural resistance to Mycobacterium bovis (BCG) in mice. J. Immunol. 127, 2417–2422.
Guilloteau, L.A., Dornand, J., Gross, A., Olivier, M., Cortade, F., Vern, Y.L., Kerboeuf, D., 2003. Nramp1 is not a major determinant in the control of *Brucella melitensis* infection in mice. Infect. Immun. 71 (2), 621–628.
Gwida, M., Dahouk, S.A., Melzer1, F., Rösler, U., Neubauer, H., Tomaso, H., 2010. Brucellosis – regionally emerging zoonotic disease? Croat. Med. J. 51, 289–295.
Hosang, K., Knoke, I., Klaudiny, J., Wempe, F., Wuttke, W., Scheit, K.H., 1994. Porcine luteal cells express monocyte chemoattractant protein-1 (MCP-1): analysis by polymerase chain reaction and cDNA cloning. Biochem. Biophys. Res. Commun. 199 (2), 962–968.
Ip, W.K., Wong, C.K., Lam, C.W., 2006. Interleukin (IL)-4 and IL-13 upregulate monocyte hemoattractant protein-1 expression in human bronchial epithelial cells: involvement of p38 mitogenactivated protein kinase, extracellular signal-regulated kinase 1/2 and Janus kinase-2 but not c-Jun NH2-terminal kinase 1/2 signalling pathways. Clin. Exp. Immunol. 145, 162–172.
Karaoglan, I., Pehlivan, S., Namiduru, M., Pehlivan, M., Kilinçarslan, C., Balkan, Y., Baydar, I., 2009. TNF-alpha, TGF-beta, IL-10, IL-6 and IFN-gamma gene polymorphisms as risk factors for brucellosis. New Microbiol. Apr. 32 (2), 173–178.
Kumar, N., Mitra, A., Ganguly, I., Singh, R., Deb, S.M., Srivastava, S.K., Sharma, A., 2005. Lack of association of brucellosis resistance with $(GT)_{13}$ microsatellite allele at 3′UTR of NRAMP1 gene in Indian zebu (*Bos indicus*) and crossbred (*B. indicus* × *B. taurus*) cattle. Vet. Microbiol. 111, 139–143.
Lang, T., Prina, E., Sibthorpe, D., Blackwell, J.M., 1997. Nramp1 transfection transfers Ity/Lsh/Bcg-related pleiotropic effects on macrophage activation: influence on antigen processing and presentation. Infect. Immun. 65 (2), 380–386.
Livak, K.J., Schmittgen, T.D., 2001. Analysis of relative gene expression data using real-time quantitative PCR and the $2^{-\Delta\Delta C}{}_T$ method. Methods 25, 402–408.
López-urrutia, L., Alonso, A., Nieto, M.L., Bayo'n, Y., Orduna, A., Crespo, M.S., 2000. Lipopolysaccharides of *Brucella abortus* and *Brucella melitensis* induce nitric oxide synthesis in rat peritoneal macrophages. Infect. Immun. 68 (3), 1740–1745.
Martins-Green, M., 2001. Int. J. Biochem. Cell Biol. 33, 427–432.
Mikeska, T., Dobrovic, A., 2009. Validation of a primer optimisation matrix to improve the performance of reverse transcription – quantitative real-time PCR assays. BMC Res. Notes 2, 112.
Namiki, M., Kawashima, S., Yamashita, T., Ozaki, M., Hirase, T., Ishida, T., Inoue, N., Hirata, K., Matsukawa, A., Morishita, R., Kaneda, Y., Yokoyama, M., 2002. Local overexpression of monocyte chemoattractant protein-1 at vessel wall induces infiltration of macrophages and formation of atherosclerotic lesion: synergism with hypercholesterolemia. Arterioscler. Thromb. Vasc. Biol. 22, 115–120.
OIE Manual, 2004. Manual of Diagnostic Tests and Vaccines for Terrestrial Animals. Bovine brucellosis. OIE, Paris, chapter 2.3.1, pp 409–438.
Paixao, T.A., Poester, F.P., Carvalho Neta, A.V., Borges, A.M., Lage, A.P., Santos, R.L., 2007. NRAMP1 3′ untranslated region polymorphisms are not associated with natural resistance to *Brucella abortus* in cattle. Infect. Immun. 75, 2493–2499.
Petersen, T.H., Brunak, S., Heijne, G., Nielsn, H., 2011. SignalP 4.0: discriminating signal peptides from transmembrane regions. Nat. Methods 8, 785–786.
Plant, J., Glynn, A.A., 1974. Natural resistance to Salmonella infection, delayed hypersensitivity and Ir genes in different strains of mice. Nature 248, 345–347.
Rafiei, A., Hajilooi, M., Shakib, R.J., Shams, S., Sheikh, N., 2006. Association between the Phe206Leu polymorphism of L-selectin and brucellosis. J. Med. Microbiol. 55 (5), 511–516.
Rafiei, A., Hajilooi, M., Vahedi, M., Shakib, R.J., 2007. The Ser128Arg polymorphism for E-selectin gene and brucellosis. Infect. Genet. Evol. 7 (4), 494–498.
Rajaravindra, K., 2008. Expression profiling of candidate genes influencing host resistance against brucellosis using invitro challenge study in reverine buffalo. Thesis. Submitted to IVRI, Izatnagar, Bareilly, India.
Rezazadeh, M., Hajilooi, M., Rafiei, A., Haidari, M., Nikoopour, E., Keramat, F., Mamani, M., Ranjbar, M., Hashemi, H., 2006. TLR4 polymorphism in Iranian patients with brucellosis. J. Infect. 53 (3), 206–210.
Rodríguez-Sanabria, F., Rull, A., Beltrán-Debón, R., Aragonès, G., Camps, J., Mackness, B., Mackness, M., Joven, J., 2010. Tissue distribution and expression of paraoxonases and chemokines in mouse: the ubiquitous and joint localisation suggest a systemic and coordinated role. J. Mol. Histol. 2010 41 (6), 379–386.
Ruggiero, P., Flati, S., Vito Di, C., Maurizi, G., Macchia, G., Facchin, A., Anacardio, R., Maras, A., Lucarelli, M., Boraschi, D., 2003. Glycosylation enhances functional stability of the chemotactic cytokine CCL2. Eur. Cytokine Netw. 14, 91–96, n(2).
Sambrook, J., Fritsch, E.F., Maniatis, T., 1989. Molecular Cloning: A Laboratory Manual, vol. 3. Cold Spring Harbour Library Press, New York, USA, pp. 6.3–6.4.
Skamene, E., Gros, P., Forget, A., Kongshavn, P.A.L., St. Charles, C., Taylor, B.A., 1982. Genetic regulation of resistance to intracellular pathogens. Nature 297, 506–509.
Spoettl, T., Hausmann, M., Herlyn, M., Gunckel, M., Dirmeier, A., Falk, W., Herfarth, H., Schoelmerich, J., Rogler, G., 2006. Monocyte chemoattractant protein-1 (MCP-1) inhibits the intestinal-like differentiation of monocytes. Clin. Exp. Immunol. 145, 190–199.
Tamura, K., Dudley, J., Nei, M., Kumar, S., 2007. MEGA4: molecular evolutionary genetics analysis (MEGA) software version 4.0. Mol. Biol. Evol. 24, 1596–1599.
Tan, H.Y., Ng, T.W., 2008. Accurate step wedge calibration for densitometry of electrophoresis gels. Opt. Commun. 281, 3013–3017.
Vakili, J., Ständker, L., Detheux, M., Vassart, G., Forssmann, W.G., Parmentier, M., 2001. J. Immunol. 167, 3406–3413.
Valdez, Y., Grassl, G.A., Guttman, J.A., Coburn, B., Gros, P., Vallance, B.A., Finlay, B., 2008. Nramp1 drives an accelerated inflammatory response during Salmonella induced colitis in mice. Cell Microbiol. 11, 351–362.
Wang, M.H., Cox, G.W., Yoshimura, T., Sheffler, L.A., Skeel, A., Leonard, E.J., 1994. Macrophage-stimulating protein inhibits induction of nitric oxide production by endotoxin- or cytokine-stimulated mouse macrophages. J. Biol. Chem. 269 (19), 14027–14031.
Wempe, F., Henschen, A., Scheit, K.H., 1991. Gene expression and cDNA cloning identified a major basic protein constituent of bovine seminal plasma as bovine monocyte chemoattractant protein-1 (MCP-1). DNA cell Biol. 10 (9), 671–679.
Wempe, F., Kuhlmann, J.K., Scheit, K.H., 1994. Characterization of the bovine monocyte chemoattractant protein-1 gene. Biochem. Biophys. Res. Commun. 202 (3), 1272–1279.
Yang, Z., Nielsen, R., Goldman, N., Pedersen, A.M., 2000. Codon-substitution models for heterogeneous selection pressure at amino acid sites. Genetics 155 (1), 431–449.
Yao, Y., Tsirka, S.E., 2010. The C terminus of mouse monocyte chemoattractant protein 1 (MCP1) mediates MCP1 dimerization while blocking its chemotactic potency. J. Biol. Chem. 285 (41), 31509–31516.
Yoshimura, T., 1993. cDNA cloning of Guinea pig monocyte chemoattractant protein-1 and expression of the recombinant protein. J. Immun. 150, 5025–5032.
Yoshimura, T., Takeya, M., Takahashi, K., 1991. Molecular cloning of rat monocyte chemoattractant protein-1 (MCP-1) and its expression in rat spleen cells and tumour cell lines. Biochem. Biophys. Res. Commun. 174 (2), 504–509.
Yoshimura, T., Yuhki, N., 1991. Neutrophil attractant/activation protein-1 and monocyte chemoattractant protein-1 in rabbit. J. Immun. 146 (10), 3483–3488.
Yoshimura, T., Yuhki, N., Moore, S.K., Appella, E., Lerman, M.I., Leonard, E.J., 1989. Human monocyte chemoattractant protein-1 (MCP-1): full-length cDNA cloning, expression in mitogen-stimulated blood mononuclear leukocytes, and sequence similarity to mouse competence gene JE. FEBS Lett. 244, 487–493.
Zhang, Y., Ernst, C.A., Rollins, B.J., 1996. Methods 10, 93–103.